# Simple and Patlak Models for Myocardial Blood Flow Measurements with Nitrogen-13-Ammonia and PET in Humans

Shinobu Kitsukawa, Katsuya Yoshida, Nizar Mullani, Keiichi Nakagawa, Kazuhiro Shimada, Akira Takami, Toshiharu Himi and Yoshiaki Masuda

*Third Department of Internal Medicine, Chiba University, and Section of Clinical Research, Division of Advanced Technology for Medical Imaging, National Institute of Radiological Sciences, Chiba, Japan; and Division of Cardiology, Department of Internal Medicine, University of Texas Medical School, Houston, Texas*

The Simple and Patlak models for estimating myocardial blood flow with $^{13}$N-ammonia have become attractive for clinical applications with PET because of their simplicity and ease of implementation. However, these models are sensitive to factors such as the data acquisition times and data integration times, which can cause errors in the estimation of myocardial blood flow, as demonstrated in this study. Limiting the application of these models to specific conditions can minimize the errors. **Methods:** Dynamic PET images of the uptake of $^{13}$N-ammonia in the heart were obtained in seven humans under rest and dipyridamole stress. Myocardial blood flow was estimated using the Simple and Patlak models for different data acquisition times and data integration times. Blood flow values were compared to flow values computed with the two-compartment model as a reference. **Results:** Blood flow values calculated with the Simple and Patlak models during the first 2 min of data acquisition were closely correlated to the two-compartment model values. Longer acquisition times resulted in significant underestimation of blood flow for the Simple model. Long integration times of greater than 60 sec also resulted in significant underestimation of blood flow for both models. **Conclusion:** The Simple and Patlak models produce estimates of myocardial blood flow that are well correlated with the two-compartment model estimated blood flows for the integration time of 60 sec from 60 to 120 sec postinjection. Because of the errors associated with longer data acquisition times and longer integration times, use of these models should be limited to a well-documented data acquisition paradigm.

**Key Words:** PET; myocardial blood flow; nitrogen-13-ammonia; Patlak model; Simple model

**J Nucl Med 1998; 39:1123–1128**

The Simple (*1*) and Patlak (*2*) models for estimating myocardial blood flow with $^{13}$N-ammonia and PET are attractive for application in humans because of their simplicity and ease of implementation. Previous animal and clinical studies with $^{13}$N-ammonia and PET have demonstrated quantitation of myocardial blood flow (MBF), and several different models have been proposed to quantitate MBF (*1–12*). The recent simplifications of the models for $^{13}$N-ammonia and PET by Yoshida et al. (*1*) for the Simple model and the graphical analysis model of Patlak validated by Choi et al. (*2*) have gained importance because of their simplicity. However, these models are based on some implicit assumptions that can result in errors in estimation of MBF if the models are not applied correctly. The length of data acquisition duration is one factor that can lead to errors in the models, as discussed by Mullani et al. (*13*) and Choi et al. (*14*). Egress of $^{13}$N radioactivity from the myocardium during data acquisition is another possible explanation for the errors. The time at which flow is calculated after a bolus injection can also contribute to underestimation of flow (*2,5,9,15*). The exact causes of these errors have not been established, but there is reasonable cause to believe that significant underestimation of blood flow occurs with longer duration of data acquisition.

In this study, we investigated the errors in MBF values in humans for different data acquisition times after the bolus injection and the influence of data acquisition durations for the Simple and Patlak models. These MBF values were compared with those calculated by the two-compartment model.

## MATERIALS AND METHODS

### Subjects

Seven human subjects (1 woman, 6 men; age range 30–72 yr; mean age 49.8 yr) were imaged with PET and $^{13}$N-ammonia. The study population included two normal healthy volunteers, two patients with angina pectoris who underwent percutaneous transluminal coronary angioplasty and who had no residual coronary artery stenosis and three patients who had chest pain without coronary artery stenosis. Informed consent was obtained for each patient before the study.

### PET

PET studies were performed with the whole-body Positologica-II positron tomography (Hitachi Medical Co., Tokyo, Japan) (*16*). This device produces five simultaneous slices separated by 18 mm. The tomographic data were collected and reconstructed on a 128 × 128 matrix, with a spatial resolution of 13 mm (FWHM) and slice thickness of 13 mm (FWHM) for the in-plane slices and 10 mm (FWHM) for the cross-plane slices. A 15-min transmission scan was acquired before the $^{13}$N-ammonia scans with a $^{68}$Ge/$^{68}$Ga external source for subsequent photon attenuation correction.

A bolus of 7–10 mCi of $^{13}$N-ammonia contained in 2–5 ml of saline solution was injected intravenously via the antecubital vein with a 15- to 20-ml saline flush. Data were acquired in the dynamic mode with two sets of images collected for each injection. An initial set of 20 dynamic images of 5.5-sec duration was first acquired and then followed by 6 images of 30-sec duration each. The total time of data acquisition for each scan was 300 sec.

Rest and stress scans were acquired for each patient. The stress scan was initiated 50–60 min after the rest study. Dipyridamole (0.56 mg/kg) was infused intravenously for 4 min and 2 min after the end of the infusion; a second dose of $^{13}$N-ammonia was injected for the stress scan.

### Estimation of Spillover by Blood-Pool Imaging

To improve the correction of spillover fraction in the flow models, we measured the spillover in the myocardium by imaging

Received May 23, 1997; revision accepted Oct. 13, 1997.

For correspondence or reprints contact: Katsuya Yoshida, MD, Section of Clinical Research, Division of Advanced Technology for Medical Imaging, National Institute of Radiological Sciences, Anagawa 4-9-1, Inage-ku, Chiba-shi, 263, Japan.

the blood pool labeled with $^{11}$CO. Four patients with angina pectoris or old myocardial infarction were imaged with $^{11}$CO and $^{13}$N-ammonia PET. Ten to 12 myocardial regions of interest (ROIs) were drawn at the midventricular level of the heart imaged with $^{13}$N-ammonia and then copied to the blood-pool image. PET-measured blood concentrations were obtained by drawing ROIs in the center of the left ventriculum. The spillover fraction was calculated by measuring the activity in the myocardial regions from the blood-pool activity in the left ventriculum during the $^{11}$CO scan. An average value of 0.28 ± 0.08 for the spillover fraction was obtained for all regions, except the septum and infarcted areas, which were excluded from the analysis.

### Image Processing

Nine to 14 ROIs with an area of 0.52 cm$^2$ each were drawn on the left ventricular myocardium at the midventricular level. ROIs were drawn on the last images of uptake and then projected to the early dynamic images for the generation of time-activity curves. Partial volume effects were corrected with a recovery coefficient of 0.65, assuming a myocardial wall thickness of 1.1 cm (*17*). Spillover of activity from the blood pool to the left myocardium was corrected with a spillover fraction of 0.28, as described earlier. All regional myocardial time activities except the septum were averaged to reduce the statistical noise with dynamic images.

Arterial blood concentration was obtained from the left atrium. An ROI was placed in the center of the left atrial cavity with an area of 0.92 cm$^2$ during the early images (*18*). These ROIs were copied to subsequent images for the generation of time-activity curves. The arterial input function was corrected for $^{13}$N metabolites from the data published by Rosenspire et al. (*19*).

### Calculation of Myocardial Blood Flow

MBF values at rest and during pharmacologic stress were calculated using the Simple flow model, Patlak graphical analysis and the two-compartment model. A brief review of the three models is presented below.

### Simple Flow Model

For partially extracted radiotracers that are trapped in tissue, flow can be obtained by using the following equation:

$$F = \frac{Cm(t)}{E \times g \times \int_0^t Ca(x)dx}, \quad \text{Eq. 1}$$

where E is the extraction fraction of $^{13}$N-ammonia and F is the MBF (ml/min/g). Cm(t) and Ca(t) are $^{13}$N activity concentrations in the myocardium and arterial blood concentrations at time t, and g is the specific gravity of myocardium (1.05 g/ml) (*20,21*). Schelbert et al. (*3*) measured the extraction fraction of $^{13}$N-ammonia for the heart in open-chest dogs and found that the relationship between flow and extraction could be defined by the following equation:

$$E = 1 - 0.607e^{(-1.25/F)}. \quad \text{Eq. 2}$$

MBF values were obtained from a lookup table of MBF versus extraction fraction generated using Equation 2 (*1,22*).

### Two-Compartment Model

The kinetic properties of $^{13}$N-ammonia in myocardial tissue can be described in terms of a functional two-compartment model in which the two compartments are the trapped and the free space (Fig. 1) (*1,6–8,23*). The rate of radioactivity change in the free compartment and that in the trapped compartment can be described by the following equations (*6,7*):

$$\frac{d}{dt}QF(t) = -[(K1 + F) \times QF(t)]/V + k2 \times QT(t) + F \times Ca(t), \quad \text{Eq. 3}$$

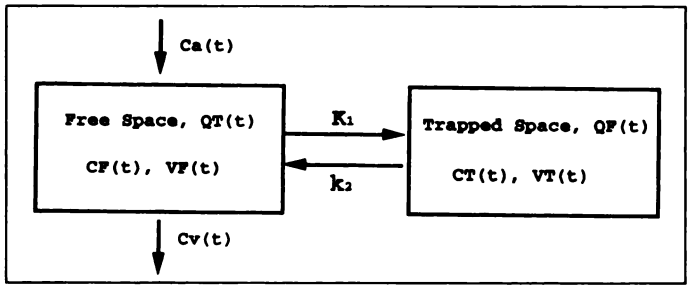


**FIGURE 1.** Two-compartment model describing myocardial kinetics of $^{13}$N-ammonia. K1 and k2 reflect tracer exchange between free and trapped space.

and

$$\frac{d}{dt}QT(t) = [K1 \times QF(t)]/V - k2 \times QT(t), \quad \text{Eq. 4}$$

where K1 (ml/min/g) and k2 (/min) represent the forward and reverse rates, respectively, for exchange between these two compartments. Krivokapich et al. (*6*) and Kuhle et al. (*7*) simplified this equation using the following assumptions. k2 is assumed to be 0 during the first 110 sec, and the venous egress is modeled by including V (ml/g), where V is the volume of distribution for free $^{13}$N-ammonia and is fixed at 0.8 ml/g. Ca(t) is the blood-pool $^{13}$N activity.

K1 is assumed to be a function of MBF. Therefore, the following relationship between K1, F and E is obtained:

$$E = K1/(K1 + F). \quad \text{Eq. 5}$$

Using Equations 2 and 5, K1 can be calculated as follows:

$$K1 = (F/0.607)e^{(1.25/F)} - F. \quad \text{Eq. 6}$$

Using the above assumptions, only one variable (MBF) needs to be estimated. Only the first 110 sec of data were used for the calculation of MBF by the two-compartment model that was developed using the BMDP software (BMDP Statistical Software Inc., Los Angeles, CA).

### Patlak Graphical Analysis

The Patlak graphical analysis can be applied to estimate MBF, as described by Choi et al. (*2*). This analysis is also based on a functional two-compartment model. The dynamic myocardial and arterial data obtained from 45 to 110 sec after $^{13}$N-ammonia injection were used to generate the following Patlak equation:

$$\frac{Qi(t)}{Ca(t)} = K\frac{\int_0^t Ca(x)dx}{Ca(t)} + \frac{MBF^2V}{(MBF + K_1)^2} + SP_{bt}\frac{AB(t)}{Ca(t)}, \quad \text{Eq. 7}$$

where AB(t) is $^{13}$N radioactivity in arterial blood and SPbt is spillover of activity from the blood pool to the myocardium. K is the slope of the straight portion of the Patlak plot and is expressed as follows:

$$K = F \times K1/(F + K1). \quad \text{Eq. 8}$$

Using Equations 6 and 8, K is expressed as follows:

$$K = F[1 - 0.607e^{-1.25/F})]. \quad \text{Eq. 9}$$

## RESULTS

An example of the time-activity curves of the uptake of $^{13}$N-ammonia in the myocardium and the blood-pool concentrations in the left atrium during a rest scan is shown in Figure 2. The averaged MBF calculated using the two-compartment model and the Simple flow model at 58, 74, 91, 107 and 285 sec

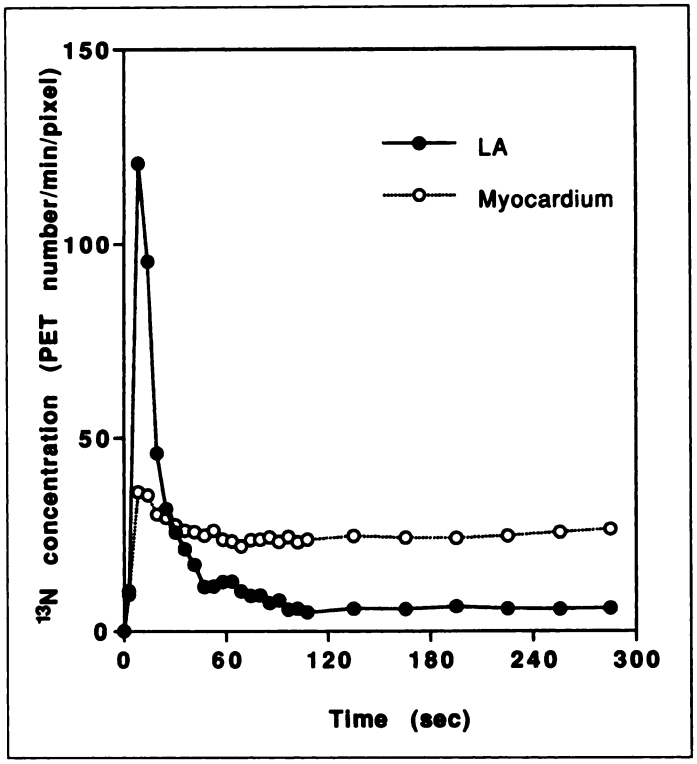


**FIGURE 2.** Time-activity curves for left atrial and left ventricular myocardium derived from dynamic $^{13}$N-ammonia PET images.

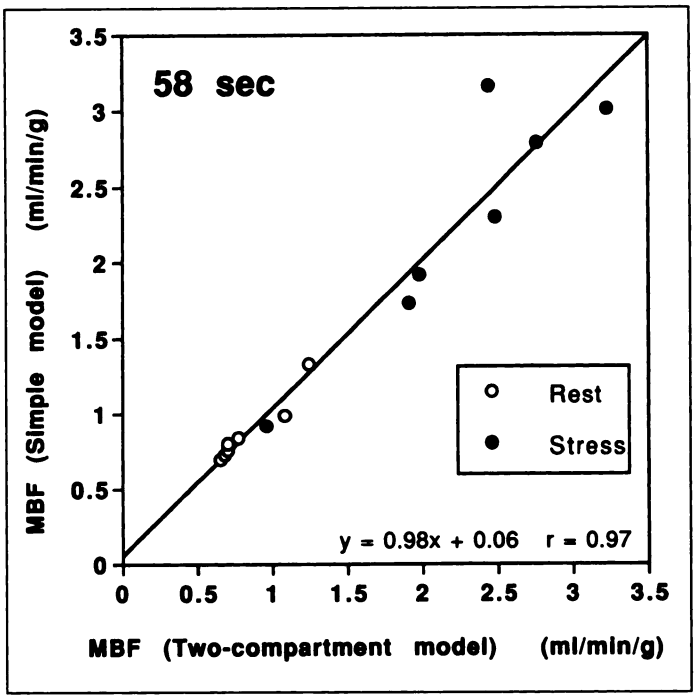


**FIGURE 4.** Correlation between myocardial blood flow (MBF) calculated by two-compartment model and by Simple model using 58-sec acquisition time.

after the bolus injection of $^{13}$N-ammonia for the data integration time of 5.5 sec each, except for the 285-sec frame, which used 30-sec integration, are shown in Figure 3. The averaged rest and stress MBF were 0.88 ± 0.22 and 2.26 ± 0.80 ml/min/g by the Simple model at 58 sec, and 0.89 ± 0.23 and 2.23 ± 0.68 ml/min/g by the two-compartment model. MBF calculated at 58 sec postinjection for all patients during rest and stress is plotted against the two-compartment model derived MBF, as shown in Figure 4. The slopes and intercepts for the linear regressions of the flow measurements computed using the Simple and the two-compartment models for the above data acquisition times are presented in Table 1. The slope value decreased from 0.98 to 0.43 in the Simple model as the data acquisition time was increased from 58 to 285 sec. The averaged MBF computed with the Simple model also decreased as the time of data acquisition was increased. Coronary flow reserve (CFR) values computed by dividing stress flow by rest flow with these models were less sensitive to the errors because of the systematic decrease in the blood flow values introduced in both the rest and stress scans, as shown in Figure 5.

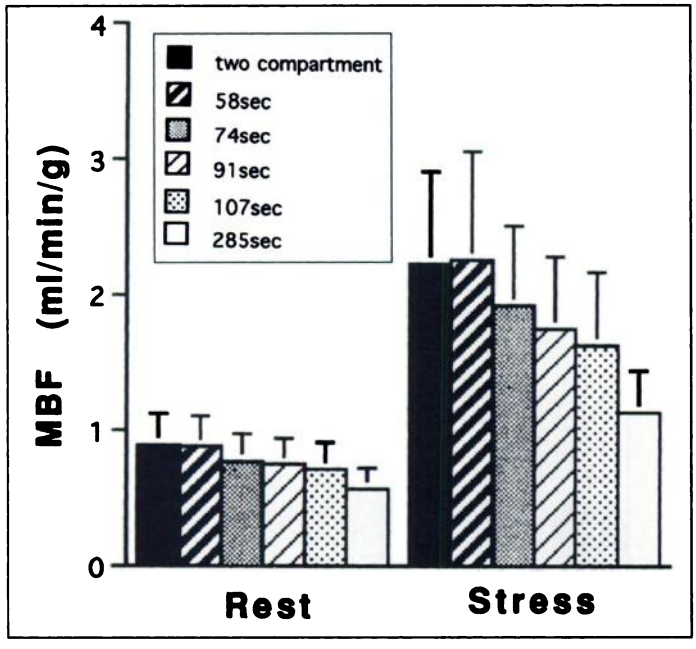


**FIGURE 3.** Myocardial blood flow (MBF) by two-compartment model and effects of acquisition time on MBF by Simple model during rest and stress.

The effect of the duration of data integration for the Simple model was explored by computing the MBF for the two-data integration time. The averaged rest and stress MBFs computed from 45 to 110 sec and from 45 to 285 sec of data acquisition are shown in Figure 6A. The averaged rest and stress MBFs computed using the Patlak model for data acquisition from 45 to 110 sec were found to be 0.83 ± 0.20 and 2.04 ± 0.58 ml/min/g. The effect of longer time for data acquisition with the model was also investigated for the time interval from 45 to 285 sec, as shown in Figure 6B. Both the Simple and Patlak models showed greatly decreased blood flow as the duration of the data integration was increased from 65 to 240 sec. This decrease in blood flow became worse at high flows measured at stress for both models. CFRs were less sensitive to the errors, as shown in Figure 7, due to the systematic underestimation of MBF for rest and stress.

**TABLE 1**
Linear Regressions of Flow Values by Simple and Two-Compartment Models

| | Data acquisition time (sec) | | | | |
|---|---|---|---|---|---|
| | 58 | 74 | 91 | 107 | 285 |
| Slope | 0.98 | 0.79 | 0.71 | 0.68 | 0.43 |
| Intercept | 0.06 | 0.13 | 0.15 | 0.13 | 0.19 |

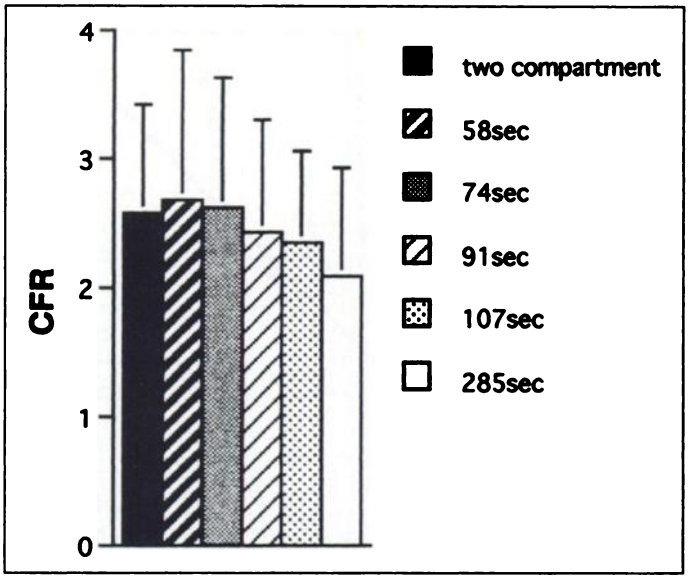


**FIGURE 5.** Coronary flow reserve (CFR) by two-compartment model and effects of acquisition time on CFR by Simple model.

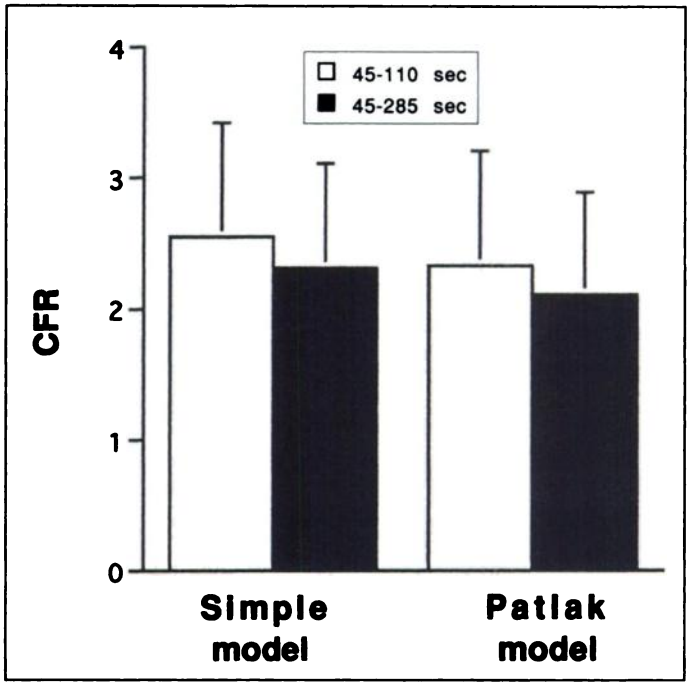


**FIGURE 7.** Effects of data integration time on coronary flow reserve (CFR) by Simple and Patlak models.

## DISCUSSION

### Decrease in Blood Flow Values as a Function of Time of Data Acquisition and Integration Time

The dynamic data acquisition results with the Simple model and the short data integration time of 5.5 sec show a gradually decreasing value of blood flow as the flow computation time is increased. A similar change in blood flow measurements in animals was presented by Nienaber et al. (*5*) using longer integration times for three different time points of 60, 210 and 510 sec after injection of tracer. Yoshida et al. (*15*), using $^{13}$N-ammonia and PET, showed a progressive decrease in blood flow as a function of data acquisition time in hypertrophic hearts in humans.

Our results also show that the longer integration times cause a decrease in blood flow with the Simple and Patlak models. This decrease was demonstrated by Choi et al. (*2*) for the Patlak method as the analysis time was increased from 70 to 120 sec to 70 to 210 sec. They showed a 29% change in the linear regression slope between the Patlak method-measured blood flow and the two-compartment model-measured blood flow for the longer duration of scan time.

Tadamura et al. (*9*) compared the Simple model to the Patlak model and found a good correlation between the two methods. They fixed the Patlak analysis time and varied the time of flow computation of the Simple model. As expected, they found a range of regression slope values and determined that one fixed time produced a good correlation. However, because both methods exhibited a decrease in blood flow as a function of time it is possible that the two methods correlated well at one time due to the linked decrease in both techniques.

The results of computing the average rest and stress blood flows with the Simple and Patlak models show that the underestimation of blood flow is made worse at higher blood flows observed during stress. This could have an important effect on the errors observed with the two methods. The effect of this error is to reduce the computed CFR values for longer data acquisition and integration times.

### The Cause of Underestimation of Blood Flow

The cause of the underestimation of blood flow by the two models as a function of time of analysis was discussed by Mullani (*13*) and Choi et al. (*14*). The major argument made by Mullani was that the assumption of negligible egress of the labeled activity from the myocardium is not true and, therefore, the assumption of negligible egress is not valid for the Simple or the Patlak models as they apply to $^{13}$N-ammonia in the heart. If the egress is not zero, then as time progresses, there will be

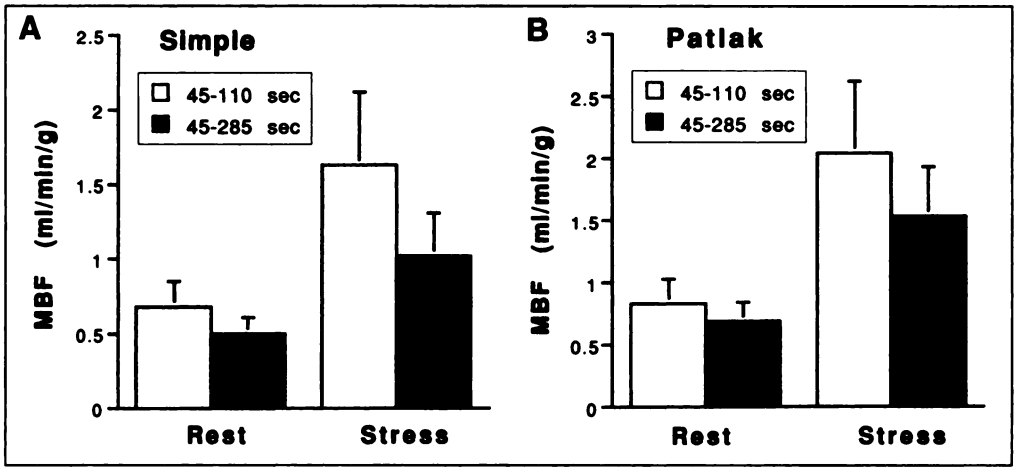


**FIGURE 6.** (A) Effects of data integration time on myocardial blood flow (MBF) by Simple model during rest and stress. (B) Effects of data integration time on MBF by Patlak graphical analysis during rest and stress.

a larger amount of labeled activity escaping from the myocardium that will result in underestimation of uptake of $^{13}$N-ammonia in the heart. Choi et al. (*14*) argued that there was less than 2% egress from the heart muscle of labeled $^{13}$N-ammonia within the first 2 min after the injection of the tracer. They explained that the underestimation of blood flow with the longer time duration of analysis with the Patlak method in their original article (*2*) was due to inaccurate estimation of arterial blood concentrations and incorrect spillover corrections or incorrect metabolite corrections. So, we have three possible causes of blood flow underestimation:

1. Inaccurate arterial sampling;
2. Inaccurate estimate of recirculating metabolites; and
3. Egress of tracer from the regions.

### Errors Due to Arterial Blood Concentration Measurement

The arterial tracer concentrations can be obtained by assigning an ROI within the left atrial or left ventricular cavity. Several articles described good results with the left atrium or the left ventricle ROI (*18,24,25*), although both have advantages and disadvantages, as discussed by Yoshida et al. (*18*) and Herrero et al. (*24*). We reported that partial volume and spillover effects can be minimized by assigning an ROI to the left atrium (*18*). We also used the spillover fraction obtained in a separate study using the carbon monoxide blood-pool labeling technique that has been used in the measurement of blood flow with $H_2{}^{15}O$ (*26*) and has been documented to be accurate. Thus, the errors due to arterial blood sampling and spillover in our study have been minimized.

### Errors Due to Recirculating Metabolites

The correction for metabolites was estimated from the articles by Rosenspire et al. (*19*) and Bormans et al. (*27*) and applied to our data. Their data showed that $<10\%$ of the recirculating labeled activity is in the form of metabolites in the first 2 min after injection.

Higher than reported levels of metabolites circulating in the blood will cause an increase in the arterial concentration of $^{13}$N-labeled metabolites, which will then reduce the value of the blood flow computed by the two models. Our data show that the blood flow value estimated at 107 sec with the Simple model is 0.71 ml/min/g, compared with 0.88 ml/min/g at 58 sec. If this reduction in blood flow is caused by the recirculating metabolites after the corrections are applied, then the levels of metabolites will need to be significantly higher than those reported in the literature.

### Egress of Tracer from the Free Compartment

A more plausible explanation for the decrease in blood flow is due to the egress of untrapped $^{13}$N-ammonia from the heart within the first few minutes. Krivokapich et al. (*28*) showed in isolated rabbit hearts that the time-activity curve for intracoronary artery injection of $^{13}$N-ammonia could be best modeled by three exponential components with half-lives of 0.17, 0.69 and 62 min. Because there was no recirculation of radioactivity in this model, there was no interference from recirculating metabolites. Similarly, Schelbert et al. (*3*) also showed three components in the intracoronary artery injections in dog hearts that they called vascular, extravascular and metabolic. The vascular component was very fast, but the extravascular component had a 32-sec half-life, and washout of the labeled tracer was observed from this area. The metabolic component had a very long half-life of over 60 min. The myocardial time-activity curve of their intracoronary artery-injected $^{13}$N-labeled ammonia showed a gradual decrease in activity for the first few minutes after the injection. There is initially a 15%–20% drop in radioactive tracer within the first 5 min, followed by a more gradual decrease attributed to the clearance of the metabolically trapped tracer. Therefore, the egress of $^{13}$N-ammonia from the heart during the first few minutes is not negligible.

Based on these animal studies and research performed with measurement of extraction fractions of $^{42}$K-potassium chloride in dog hearts with indicator dilution techniques by Bassingthwaighte et al. (*29*), the short half-life of 0.17 min for the first component is most likely due to the vascular transit time of the bolus. The second component, which has a longer transit time of 0.5- to 0.69-min half-life, represents a larger volume of distribution in which the $^{13}$N-ammonia is freely distributed and can egress from this space. This may be the functionally free space in the tissue that has been modeled by Mullani et al. (*20*), Yoshida et al. (*1*) and Kuhle et al. (*7*). The third component has a long half-life of 62 min and is most likely due to the metabolically trapped component of the tracer.

### Time-Dependent Extraction Fraction

Unlike the microsphere model, in which the activity is trapped instantaneously in the capillaries, a part of the injected $^{13}$N-ammonia is distributed in the free compartment for the first 3–5 min. It continues to egress from the free compartment, as shown in the intracoronary injection data. This egress results in time-dependent extraction fractions demonstrated by Bassingthwaighte et al. (*29*) and mathematically derived by Mullani et al. (*20*). Extraction fraction is not constant as a function of time for nonmicrosphere-type tracers that are not injected as a bolus, such as $^{13}$N-ammonia.

The Simple and Patlak models apply a fixed value of the extraction fraction that underestimates the early extraction fraction and overestimates the late extraction fraction. To reduce the error in MBF measurements with the Simple and Patlak models, a compromise time has to be selected for the duration of the scan and the initiation of the scan after the injection of the tracer. Collecting data earlier than 58 sec could result in other errors such as large spillover from the blood pool to the myocardium and larger amounts of tracer in the free compartment. Therefore, it is our conclusion that a time interval of ~60 sec starting from ~60 sec postinjection would be a good compromise for the Simple model applied to the heart with $^{13}$N-ammonia.

### Technical Limitations

The septum was excluded from the spillover calculations and the blood flow estimations because the spillover from the right ventricle onto the septum is different from the other area of the heart. We also used a fixed recovery coefficient for partial volume correction. For the purpose of this study, we averaged all ROIs, except the septum, to minimize the errors associated with fixed spillover and partial volume corrections and reduce the statistical noise for the study. However, this analysis is not appropriate for clinical situations because the septum is as important as other regions and many cardiac patients have regional abnormalities, wall thinning and hypertrophy. Better methods of partial volume and spillover corrections are needed to overcome these limitations for clinical applications.

### Clinical Applications

The simplifications of the models for $^{13}$N-ammonia and PET have several advantages for clinical application:

1. Computation times for the Simple and Patlak models are shorter than the two-compartment analysis;
2. Only two images, an image of myocardial uptake and an image of arterial input function, are required for the

Simple model analysis, as suggested by Yoshida et al. (*1*); and

3. Smaller data files are required, dramatically reducing the image reconstruction time.

## CONCLUSION

The Simple and Patlak models do not account for the egress of radiotracer from the free compartment in the heart. Therefore, they underestimate blood flow when long scan times are used with $^{13}$N-ammonia and PET in humans. A compromise scan time of ~60-sec duration starting approximately 60 sec postinjection of tracer seems to produce reasonable blood flow values with good flow reserve numbers and may be useful for clinical application of the Simple model for use with $^{13}$N-ammonia in humans.

## ACKNOWLEDGMENTS

We thank Dr. Kazutoshi Suzuki and Kazuhiko Tamate for preparing the radiotracers $^{13}$N-ammonia and $^{11}$CO. This work was supported in part by the Japanese Special Coordination Fund for Promotion of Science and Technology.

## REFERENCES

1. Yoshida K, Mullani N, Gould KL. Coronary flow and flow reserve by PET simplified for clinical applications using rubidium-82 or nitrogen-13-ammonia. *J Nucl Med* 1996;37:1701–1712.
2. Choi Y, Huang SC, Hawkins RA, et al. A simplified method for quantification of myocardial blood flow using nitrogen-13-ammonia and dynamic PET. *J Nucl Med* 1993;34:488–497.
3. Schelbert HR, Phelps ME, Huang SC, et al. N-13 ammonia as an indicator of myocardial blood flow. *Circulation* 1981;63:1259–1272.
4. Bellina CR, Parodi O, Camici P, et al. Simultaneous in vitro and in vivo validation of nitrogen-13-ammonia for the assessment of regional myocardial blood flow. *J Nucl Med* 1990;31:1335–1343.
5. Nienaber CA, Ratib O, Gambhir SS, et al. A quantitative index of regional blood flow in canine myocardium derived noninvasively with $^{13}$N ammonia and dynamic positron emission tomography. *J Am Coll Cardiol* 1991;17:260–269.
6. Krivokapich J, Smith GT, Huang SC, et al. $^{13}$N ammonia myocardial imaging at rest and with exercise in normal volunteers: quantification of absolute myocardial perfusion with dynamic positron emission tomography. *Circulation* 1989;80:1328–1337.
7. Kuhle WG, Porenta G, Huang SC, et al. Quantification of regional myocardial blood flow using $^{13}$N-ammonia and reoriented dynamic positron emission tomographic imaging. *Circulation* 1992;86:1004–1017.
8. Endo M, Yoshida K, Iinuma TA, et al. Noninvasive quantification of regional myocardial blood flow and ammonia extraction fraction using nitrogen-13 ammonia and positron emission tomography. *Ann Nucl Med* 1987;1:1–6.
9. Tadamura E, Tamaki N, Yonekura Y, et al. Assessment of coronary vasodilation reserve by N-13 ammonia PET using the microsphere method and Patlak plot analysis. *Ann Nucl Med* 1995;9:109–118.
10. Hutchins GD, Schwaiger M, Rosenspire KC, Krivokapich J, Schelbert HR, Kuhl DE. Noninvasive quantification of regional blood flow in the human heart using N-13 ammonia and dynamic positron emission tomographic imaging. *J Am Coll Cardiol* 1990;15:1032–1042.
11. Muzik O, Beanlands RSB, Hutchins GD, Mangner TJ, Nguyen N, Schwaiger M. Validation of nitrogen-13-ammonia tracer kinetic model for quantification of myocardial blood flow using PET. *J Nucl Med* 1993;34:83–91.
12. Bol A, Melin JA, Vanoverschelde JL, et al. Direct comparison of [$^{13}$N]ammonia and [$^{15}$O]water estimates of perfusion with quantification of regional myocardial blood flow by microspheres. *Circulation* 1993;87:512–525.
13. Mullani NA. Is the Patlak graphical analysis method applicable to measurements of myocardial blood flow with nitrogen-13-ammonia? *J Nucl Med* 1993;34:1831–1832.
14. Choi Y, Huang SC, Hawkins RA, et al. Is the Patlak graphical analysis method applicable to measurements of myocardial blood flow with nitrogen-13-ammonia? *J Nucl Med* 1993;34:1832–1833.
15. Yoshida K, Endo M, Himi T, et al. Measurement of regional myocardial blood flow in hypertrophic cardiomyopathy: application of the first-pass flow model using [$^{13}$N]ammonia and PET. *Am J Physiol Imaging* 1989;4:97–104.
16. Tanaka E, Nohara N, Tomitani T, et al. A whole-body positron tomography, POSITOLOGICA-II: design and performance evaluation. In: Raynaud C, ed. *Proceedings of the Third World Congress on Nuclear Medicine and Biology, August–September 1982*, vol. 1. Paris: Pergamonn Press; 1982:535–538.
17. Hoffman EJ, Huang SC, Phelps ME. Quantitation in positron emission CT: 1. Effect of object size. *J Comput Assist Tomogr* 1979;3:299–308.
18. Yoshida K, Endo M, Fukuda H, et al. Measurement of arterial tracer concentrations from cardiac PET images. *J Comput Assist Tomogr* 1995;19:182–187.
19. Rosenspire KC, Schwaiger M, Mangner TJ, Hutchins GD, Sutorik A, Kuhl DE. Metabolic fate of [$^{13}$N]ammonia in human and canine blood. *J Nucl Med* 1990;31:163–167.
20. Mullani NA, Goldstein RA, Gould KL, et al. Myocardial perfusion with rubidium-82. I. Measurement of extraction-fraction and flow with external detectors. *J Nucl Med* 1983;24:898–906.
21. Schelbert HR, Phelps ME, Hoffman EJ, Huang SC, Selin CE, Kuhl DE. Regional myocardial perfusion assessed with N-13 labeled ammonia and positron emission tomography. *Am J Cardiol* 1979;43:209.
22. Herrero P, Markham J, Shelton ME, Weinheimer CJ, Bergmann SR. Noninvasive quantification of regional myocardial perfusion with rubidium-82 and positron emission tomography: exploration of a mathematical model. *Circulation* 1990;82:1377–1386.
23. Mullani NA, Gould KL. First-pass measurements of regional blood flow with external detectors. *J Nucl Med* 1983;24:577–581.
24. Herrero P, Hartman JJ, Senneff MJ, Bergmann SR. Effects of time discrepancies between input and myocardial time–activity curves on estimates of regional myocardial perfusion with PET. *J Nucl Med* 1988;29:241–247.
25. Weinberg IN, Huang SC, Hoffman EJ, et al. Validation of PET-acquired input functions for cardiac studies. *J Nucl Med* 1994;35:558–566.
26. Bergmann SR, Herrero P, Markham J, Weinheimer CJ, Walsh MN. Noninvasive quantitation of myocardial blood flow in human subjects with oxygen-15-labeled water and positron emission tomography. *J Am Coll Cardiol* 1989;14:639–652.
27. Bormans G, Maes A, Langendries W, et al. Metabolism of nitrogen-13 labeled ammonia in different conditions in dogs, human volunteers and transplant patients. *Eur J Nucl Med* 1995;22:116–121.
28. Krivokapich J, Huang SC, Phelps ME, MacDonald NS, Shine KI. Dependence of $^{13}NH_3$ myocardial extraction and clearance on flow and metabolism. *Am J Physiol* 1982;242:H536–H542.
29. Bassingthwaighte JB, Winkler B, King RB. Potassium and thallium uptake in dog myocardium. *J Nucl Med* 1997;38:264–274.